Histone–GFP fusion protein enables sensitive analysis of chromosome dynamics in living mammalian cells

Teru Kanda*, Kevin F. Sullivan† and Geoffrey M. Wahl*

Background: The amplification of oncogenes in cancer cells is often mediated by paired acentric chromatin bodies called double minute chromosomes (DMs), which can accumulate to a high copy number because of their autonomous replication during the DNA synthesis phase of the cell cycle and their subsequent uneven distribution to daughter cells during mitosis. The mechanisms that control DM segregation have been difficult to investigate, however, as the direct visualization of DMs in living cells has been precluded because they are far smaller than normal chromosomes. We have visualized DMs by developing a highly sensitive method for observing chromosome dynamics in living cells.

Results: The human histone H2B gene was fused to the gene encoding the green fluorescent protein (GFP) of *Aequorea victoria* and transfected into human HeLa cells to generate a stable line constitutively expressing H2B–GFP. The H2B–GFP fusion protein was incorporated into nucleosomes without affecting cell cycle progression. Using confocal microscopy, H2B–GFP allowed high-resolution imaging of both mitotic chromosomes and interphase chromatin, and the latter revealed various chromatin condensation states in live cells. Using H2B–GFP, we could directly observe DMs in living cancer cells; DMs often clustered during anaphase, and could form chromosomal 'bridges' between segregating daughter chromosomes. Cytokinesis severed DM bridges, resulting in the uneven distribution of DMs to daughter cells.

Conclusions: The H2B–GFP system allows the high-resolution imaging of chromosomes, including DMs, without compromising nuclear and chromosomal structures and has revealed the distinctive clustering behavior of DMs in mitotic cells which contributes to their asymmetric distribution to daughter cells.

Addresses: *Gene Expression Laboratory, The Salk Institute for Biological Studies, 10010 N. Torrey Pines Road, La Jolla, California 92037, USA. †Department of Cell Biology, The Scripps Research Institute, La Jolla, California 92037, USA.

Correspondence: Geoffrey M. Wahl
E-mail: wahl@salk.edu

Received: 17 December 1997
Revised: 12 February 1998
Accepted: 18 February 1998

Published: 10 March 1998

Current Biology 1998, 8:377–385
http://biomednet.com/elecref/0960982200800377

Background

In eukaryotes, segregation of sister chromatids during mitosis requires spindle fiber attachment to the kinetochores formed at centromeric DNA. Cancer cells often harbor abnormal chromosomes such as dicentric or acentric chromosomes, however, which would be expected to behave anomalously. Double minute chromosomes (DMs) are paired chromatin bodies that have been reported in as many as 50% of human tumors but have never been observed in normal cells [1,2]. As DMs lack functional centromeres, they do not segregate by the same mechanism used by normal chromosomes. DMs can accumulate to a high copy number because of their autonomous replication during the DNA synthesis (S) phase of the cell cycle and their subsequent uneven distribution to daughter cells during mitosis. As DMs contain a diversity of amplified oncogenes [3], their uneven segregation and accumulation increases the malignant potential during tumor progression. On the other hand, as DM loss can decrease tumor cell viability [4], understanding the mechanism of DM segregation could lead to the identification of highly selective anti-neoplastic agents that specifically disrupt the transmission of DMs to daughter cells.

Observations of fixed chromosomes in DM-harboring cancer cells have provided some insights into DM segregation during mitosis [5,6]. Fixation and permeabilization of cells may cause artificial distortions of chromosome distribution, however, and could perturb intracellular structures. An ideal strategy for examining the dynamics of DM segregation would involve their direct visualization in living cells. DMs vary in size, however, and many are at the size limit of conventional cytogenetics (~$1–2 \times 10^6$ bp) [2], which has prevented their detection in cycling cells. This report describes a fluorescent labeling system with sufficient sensitivity to visualize DMs *in vivo*, and that enables analyses of their segregation dynamics in real time during mitosis.

One approach to label chromosomes in living cells involves the fluorescent tagging of proteins that localize to chromosomes. The nucleosome is the fundamental repeating unit

of chromatin. Each nucleosome core particle consists of an octamer of core histones with 146 bp of micrococcal-nuclease-resistant DNA wrapped around it [7]. As histones are the principal structural proteins of eukaryotic chromosomes, they are attractive targets for fluorescent labeling. Purified calf thymus histones (H2A and H2B) conjugated with rhodamine have been microinjected into *Drosophila* embryos to analyze cell lineage relationships [8] and chromosomal condensation and decondensation events [9]. The success of this approach demonstrates the utility of fluorescently labeled histones to study chromosomal dynamics in living cells.

The green fluorescent protein (GFP) of the jellyfish *Aequorea victoria* retains its fluorescent properties when recombinant GFP proteins are expressed in eukaryotic cells [10]. GFP fusion proteins have been successfully targeted to specific subcellular organelles and structures including the nucleus, plasma membrane, mitochondrion, cytoskeleton, and Golgi apparatus [11–13]. Recently, GFP tagging also enabled visualization of specific chromosomal regions [14–16]. These results indicate the potential utility of a histone–GFP fusion protein to fluorescently label chromosomes in living cells. The feasibility of this approach is indicated by the observation that a fusion protein of GFP and yeast histone H2B localized properly in yeast nuclei [17]. Here, we show that a fusion protein of GFP and human H2B (H2B–GFP) is incorporated into nucleosome core particles without perturbing cell cycle progression. H2B–GFP bound chromosomes and DMs with high specificity, allowing them to be easily observed using a confocal microscope. We describe for the first time the behavior of DMs during mitosis in living cells. Our results reveal that DMs often cluster in anaphase cells and attach to groups of segregating chromosomes. Sometimes, segregating daughter chromosomes are connected by DM 'bridges' spanning the midplane of anaphase cells. Time-lapse observation revealed that cytokinesis severs the DM bridges, resulting in asymmetric distribution of DMs to the daughter cells.

Results

Stable expression of H2B–GFP in HeLa cells

The cDNA encoding human H2B was tagged at its carboxyl terminus with DNA encoding codon-optimized enhanced GFP [18] (Figure 1), and the chimeric gene was subcloned into a mammalian expression vector. The construct was introduced into the human HeLa cell line by transient transfection, and fluorescence microscopic observation indicated that H2B–GFP protein localized to interphase nuclei and mitotic chromosomes (data not shown). To analyze the effects of constitutive H2B–GFP expression on cell cycle progression, we transfected HeLa cells and cultured them under drug selection (blasticidin) to obtain clones that stably expressed the H2B–GFP transgene. GFP-positive colonies arose in about 10% of blasticidin-resistant colonies, while other colonies (~90%) were negative for GFP for unknown reasons. We obtained several stable cell lines expressing H2B–GFP. A cell line with uniform, high-level expression of H2B–GFP was chosen for further analyses (Figure 2). The expression level of H2B–GFP in this cell line was stable for more than three months in the absence of continuous blasticidin selection. The high degree of stability of the integrated H2B–GFP gene in the absence of selection strongly suggests that chromosome stability is unimpaired by constitutive H2B–GFP expression. The mitotic index and the growth rate of this cell line were similar to those of the

Figure 1

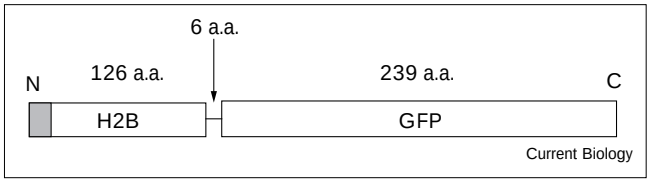

The H2B–GFP chimeric protein. The H2B protein was tagged with GFP at its carboxyl terminus; the length, in amino acids (a.a.), of each region and of the junction between H2B and GFP is indicated. The amino (N) and carboxyl (C) termini of the fusion protein are indicated and the histone amino-terminal tail is shown as a gray box.

Figure 2

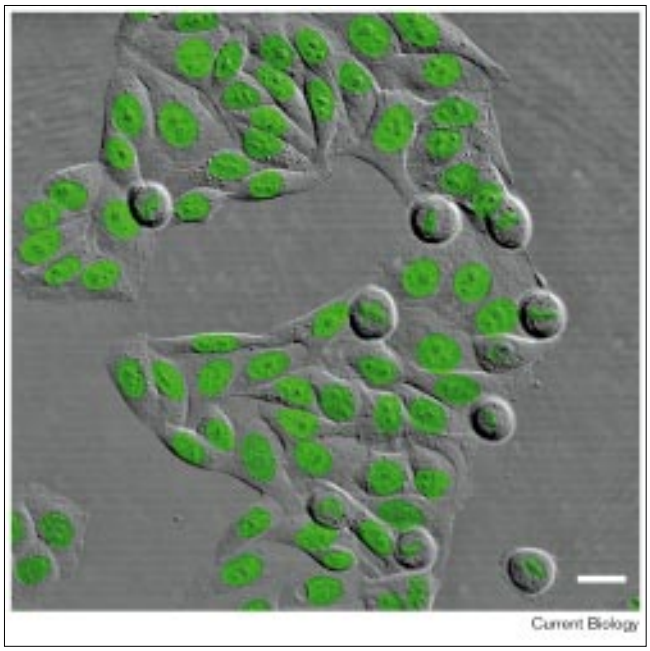

Cells expressing H2B–GFP. A confocal microscopic image of live HeLa cells constitutively expressing H2B–GFP; the GFP fluorescence (green) was overlaid onto a differential interference contrast image. The figure shows that H2B–GFP is detected highly efficiently in cells in all phases of the cell cycle and that H2B–GFP is contained solely in the nucleus. The scale bar is 25 μm.

parental HeLa cells (data not shown). We also used a cell line stably expressing a fusion protein of H2B fused at its amino terminus to GFP and got essentially the same results (data not shown).

H2B–GFP is incorporated into nucleosomes

We biochemically fractionated nucleosome core particles from cells expressing H2B–GFP and analyzed for the presence of the fusion protein to determine if it was a component of nucleosome core particles. Mononucleosomes were generated by extensive micrococcal nuclease digestion of the isolated nuclei expressing H2B–GFP (Figure 3a). Digested chromatin was pelleted by subsequent centrifugation of the nuclease-treated nuclei. The supernatant and pellet, together with whole cell lysate of HeLa cells and HeLa cells expressing H2B–GFP, were analyzed by western blotting using an anti-human-H2B antibody. The majority of the expressed H2B–GFP protein was recovered in the pelleted chromatin fraction, and little if any was detected in the supernatant (Figure 3b, compare lane 5 with lane 6). The chromatin fraction was further fractionated by sucrose gradient centrifugation in the presence of 0.5 M NaCl to dissociate histone H1 [19]. Electrophoretic analysis of the DNA showed that fractions 2 through 4 (predominantly fraction 3) contained DNA of about 146 bp (the size expected for the DNA wrapped around nucleosome core particles; Figure 3e). The proteins in the samples were analyzed by gel electrophoresis; H2B–GFP protein and core histones were identified in the mononucleosome fractions by Coomassie staining (Figure 3c). Aliquots of the same samples were analyzed by western blotting using anti-human-H2B antibody to specifically detect H2B and H2B–GFP protein (Figure 3d). The results demonstrate that the H2B–GFP fusion protein is in the mononucleosome fractions of the sucrose gradient and that its distribution parallels that of native histones in the gradient. The relative amounts of H2B–GFP and endogenous H2B in the purified mononucleosomes (Figure 3d) were comparable to their relative amounts in the whole cell lysate (Figure 3b, lane 2), suggesting that H2B–GFP protein is incorporated into nucleosomes efficiently. H2B–GFP association with the nucleosome core particle was stable under conditions that dissociate histone H1 [19], suggesting that adventitious aggregation of H2B–GFP protein with chromatin is unlikely (see Discussion).

Figure 3

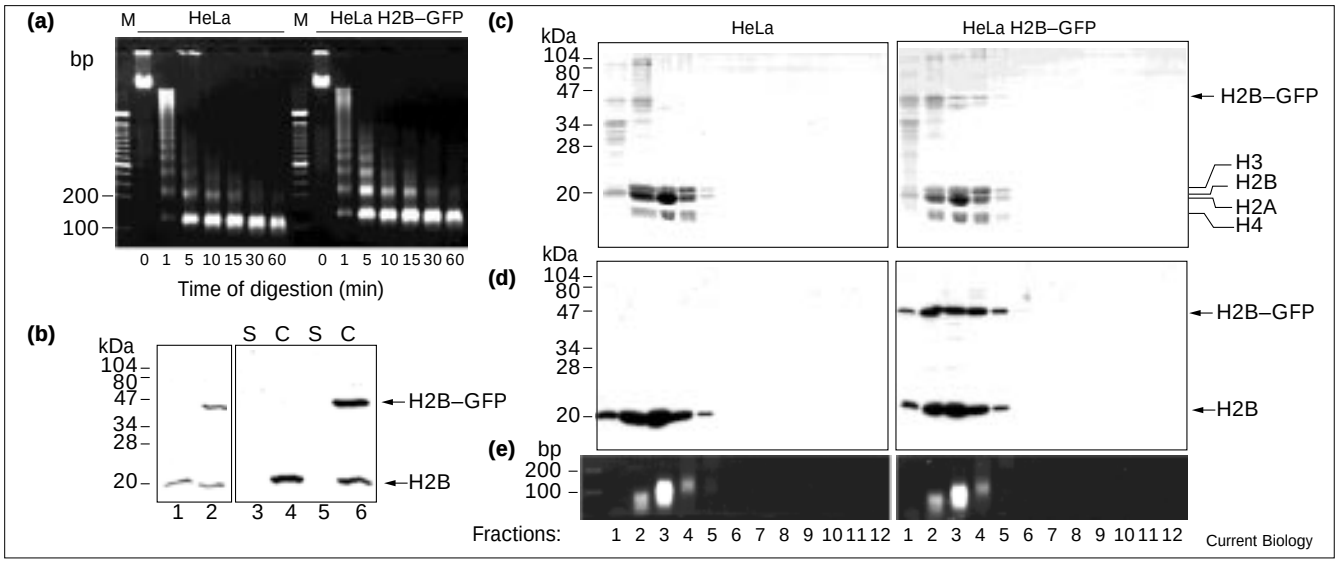

H2B–GFP is incorporated into mononucleosomes. (a) Micrococcal nuclease digestion of nuclei from HeLa cells and HeLa cells expressing H2B–GFP. Isolated nuclei were digested for 0, 1, 5, 10, 15, 30, and 60 min, as indicated, and the DNA protected from digestion by the binding of nucleosomal core proteins was analyzed by 1.5% agarose gel electrophoresis. The markers used (M) were 100 bp ladders. (b) Whole cell lysate (25 μg each from HeLa cells, lane 1, or HeLa cells expressing H2B–GFP, lane 2), supernatants (S) and soluble chromatin fractions (C) of the digested nuclei (10 μg each from HeLa cells, lanes 3 and 4, or HeLa cells expressing H2B–GFP, lanes 5 and 6) were analyzed by western blotting using anti-human-H2B antibody. Soluble chromatin fractions were prepared as described in Materials and methods. H2B–GFP protein (approximately 45 kDa) and endogenous H2B protein are indicated. (c) Sucrose gradient analysis of mononucleosome populations. The mononucleosome protein–DNA complexes from HeLa cells and HeLa cells expressing H2B–GFP, prepared by micrococcal nuclease digestion, were purified through parallel 5–30% sucrose gradients. Proteins from each fraction were extracted and analyzed by electrophoresis through SDS–15% polyacrylamide gels and Coomassie staining. H2B–GFP protein and the native core histone proteins (H2A, H2B, H3 and H4) are indicated. (d) Aliquots of the fractions in (c) were electrophoresed and analyzed by western blotting using anti-human-H2B antibody. H2B–GFP protein and endogenous H2B protein are indicated. (e) DNA in each fraction was analyzed by 1.5% agarose gel electrophoresis.

H2B–GFP incorporation does not inhibit cell cycle progression

It was conceivable that GFP tagging of H2B protein could affect chromatin structure and perturb cell cycle progression as a consequence. Therefore, the cell cycle distribution of the established cell line expressing H2B–GFP was analyzed to ascertain differences in cell cycle progression relative to the parental cell population. Asynchronous HeLa cells and the transformant expressing H2B–GFP were fixed with ethanol, stained with propidium iodide (PI), and analyzed by fluorescence-activated cell sorting (FACS). The green emission of GFP-labeled cells produced an approximately three-log shift from parental HeLa cells (Figure 4a,b). DNA content was determined by measuring the red emission of PI (Figure 4c,d). The results indicate that the cell cycle distribution of asynchronous HeLa cells expressing H2B–GFP is indistinguishable from that of the parental HeLa cells, clearly demonstrating that the H2B–GFP protein has little, if any, effect on cell cycle progression.

H2B–GFP decorates chromosomes in living cells

Cells expressing H2B–GFP were observed using confocal microscopy to determine the pattern of chromatin staining in interphase and mitosis. As shown in Figure 5, H2B–GFP enabled highly sensitive chromatin detection in all phases of the cell cycle. Fixation and permeabilization of the cells, which might cause artificial distortion of intracellular structure, was not required to obtain such images. H2B–GFP was highly specific for nuclear chromatin as no fluorescence was observed in the cytoplasm. In addition, H2B–GFP provided a remarkable level of sensitivity. For example, a chromatin structure that appeared to be a pair of lagging sister chromatids with a centromeric constriction was readily observed (Figure 5e). The fine intranuclear chromatin architecture in interphase nuclei visualized by H2B–GFP was consistent with the previously reported deconvoluted optical-sectioning images of fixed nuclei obtained by 4′,6′-diamidino-2-phenylindole (DAPI) staining [20]. Chromosome spreads of the H2B–GFP-expressing cells also showed that the GFP fluorescence patterns were identical to the patterns obtained using DAPI (Figure 5i,j).

Figure 4

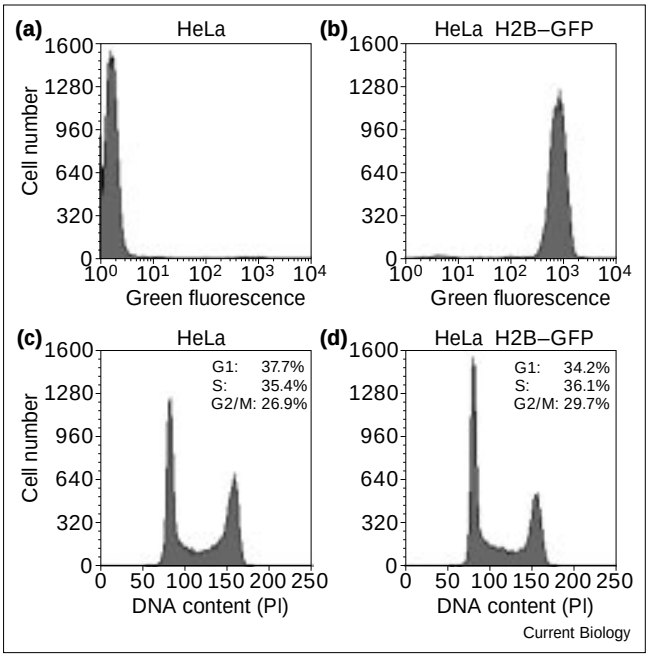

H2B–GFP expression does not affect cell cycle progression. (a,c) HeLa cells and (b,d) HeLa cells expressing H2B–GFP were fixed with ethanol, stained with PI, and analyzed by FACS. (a,b) Flow cytometry histograms of GFP fluorescence. (c,d) Flow cytometry histograms of the DNA content determined by PI staining. The estimated proportion of cells in the G1, S, and G2/M fractions are indicated.

We also observed perinucleolar regions densely stained with H2B–GFP that resembled chromocenters in interphase nuclei (Figure 5a). A previously described feature of chromocenters is that they are heterochromatic and often contain centromeres [21,22]. Double staining with centromere antibodies and H2B–GFP demonstrated that certain regions with intense H2B–GFP staining possessed multiple centromeres (Figure 6). From this result, coupled with the concordance of H2B–GFP staining and DAPI staining (Figure 5i,j), we conclude that H2B–GFP staining reflects the density of packing of DNA in different regions of the nucleus. Thus, chromosomal domains that have previously only been examined in fixed cells may be monitored using the H2B–GFP method in living cells.

Visualization of DMs in living cells

We applied our highly sensitive H2B–GFP chromatin-labeling technique to the analysis of DMs in living cells. A retroviral vector was constructed to enable the efficient transfer and expression of H2B–GFP in a broad range of host cells. We used a vesicular stomatitis virus G glycoprotein (VSV-G) pseudotyped retroviral vector to obtain high viral titers [23]. COLO320DM cells harboring DMs containing an amplified c-*myc* gene [24,25] were infected with the H2B–GFP retrovirus, and two days later over 90% of the cells expressed H2B–GFP protein. FACS analyses revealed that cell cycle progression of COLO320DM cells was not affected by H2B–GFP expression (data not shown). We collected serial-sectioning images of living COLO320DM cells expressing H2B–GFP using confocal microscopy. We noticed that small fluorescent dots were frequently observed in mitotic cells (Figure 7a,b). The sizes of these dots were 0.7–0.85 μm in diameter, corresponding to the size of DMs in this cell line. We found that they frequently associated in clusters in anaphase cells where they were attached to normal chromosomes (Figure 7a). Sometimes they aligned in regular arrays and

Figure 5

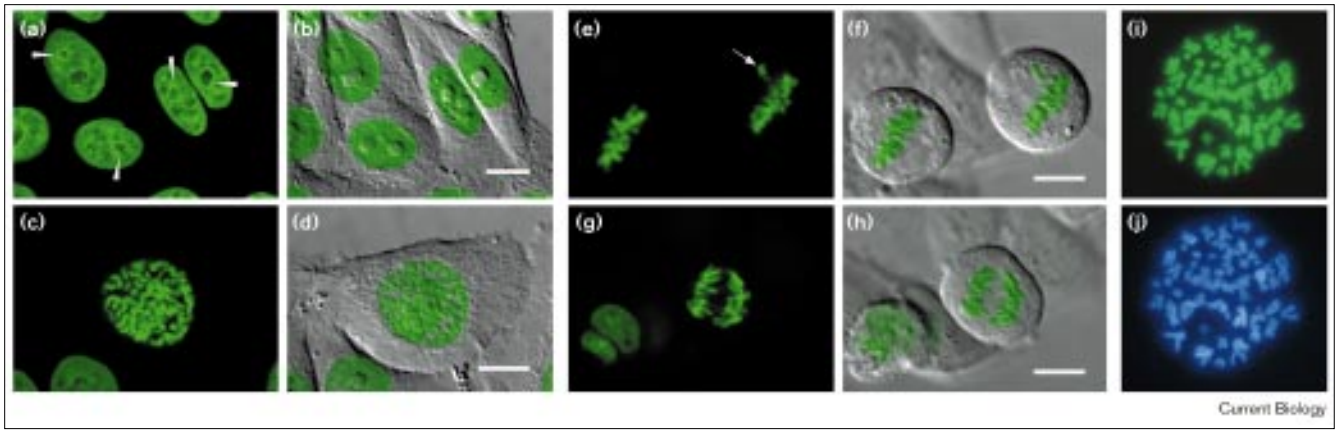

Localization of H2B–GFP protein. **(a–h)** Confocal microscopic images of live HeLa cells expressing H2B–GFP in various cell cycle phases. (a,c,e,g) The GFP fluorescence and (b,d,f,h) the corresponding differential interference contrast images are shown for (a,b) interphase, (c,d) prophase, (e,f) metaphase and (g,h) anaphase cells. Perinucleolar densely staining regions of H2B–GFP are indicated by arrowheads in (a). A pair of lagging sister chromatids with a centromeric constriction is indicated by an arrow in (e). The scale bars are 10 μm. **(i)** GFP localization and **(j)** DAPI staining of fixed chromosome spreads of HeLa cells expressing H2B–GFP.

formed an extended bridge between segregating groups of daughter chromosomes (Figure 7b).

In order to confirm that these dot-like chromatin bodies were DMs, mitotic COLO320DM cells were fixed with or without colcemid treatment, and the DM distribution was analyzed by fluorescence *in situ* hybridization (FISH) using a c-*myc* cosmid probe. Whereas chromosome spreads of colcemid-treated cells usually had dispersed DMs (Figure 7c), DMs were observed to form clusters in untreated mitotic cells (Figure 7d,e). The DMs detected using FISH were strikingly similar to the dot-like structures observed in H2B–GFP-expressing cells (compare Figure 7a,b to Figure 7d,e). The results strongly suggest that the dot-like chromatin bodies observed in living cells are DMs. We found that most of the observed mitotic cells contained clustered DMs, although the number of DMs varied from cell to cell. Approximately 30% of the anaphase cells showed bridge formations involving DMs. We therefore conclude that the clustering of DMs and their unbalanced distribution to daughter cells during mitosis are very common events in this cell line.

Figure 6

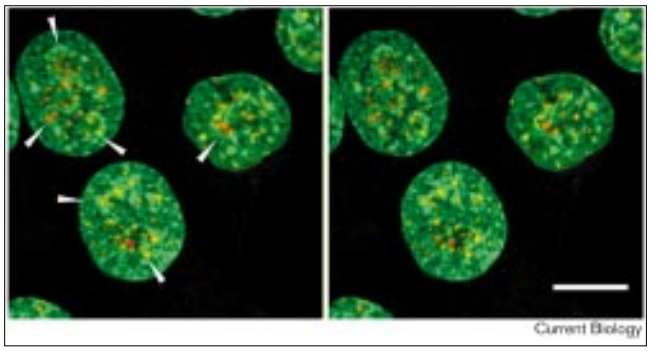

Perinucleolar regions densely stained with H2B–GFP possess multiple centromeres. Stereoscopic images of centromere localization in H2B–GFP-expressing HeLa cells. Centromeres were detected by immunofluorescence using a human anti-centromere antiserum. Localization of centromeres (red) and H2B–GFP (green) are indicated. Perinucleolar heterochromatic domains are indicated by arrowheads. The scale bar is 10 μm.

We next analyzed DM segregation by making time-lapse observations using an epifluorescence microscope (Figure 8). Clustered DMs were attached by the extended arms of normal segregating chromosomes, forming a chromosome bridge (Figure 8a). This bridge was further extended as daughter chromosomes segregated (Figure 8b). Subsequently, the bridge was severed by the process of cytokinesis (Figure 8c), and the cluster of DMs appeared to be unevenly distributed to daughter nuclei (Figure 8d). These results clearly demonstrate that DMs frequently cluster in anaphase cells, sometimes forming chromosomal bridges, and that their uneven distribution to daughter cells can result from cytokinesis severing DM bridges asymmetrically.

Discussion

We have described a novel strategy to fluorescently label chromosomes in living cells and the successful application of this strategy to observe DMs in living cells. Despite the large size of the GFP tag (239 amino acids), it has been shown in numerous cases that GFP-tagged proteins are functional and localize properly [11–13]. Such is also the case with the histone H2B–GFP fusion protein. Our experimental data demonstrate the co-fractionation of

Figure 7

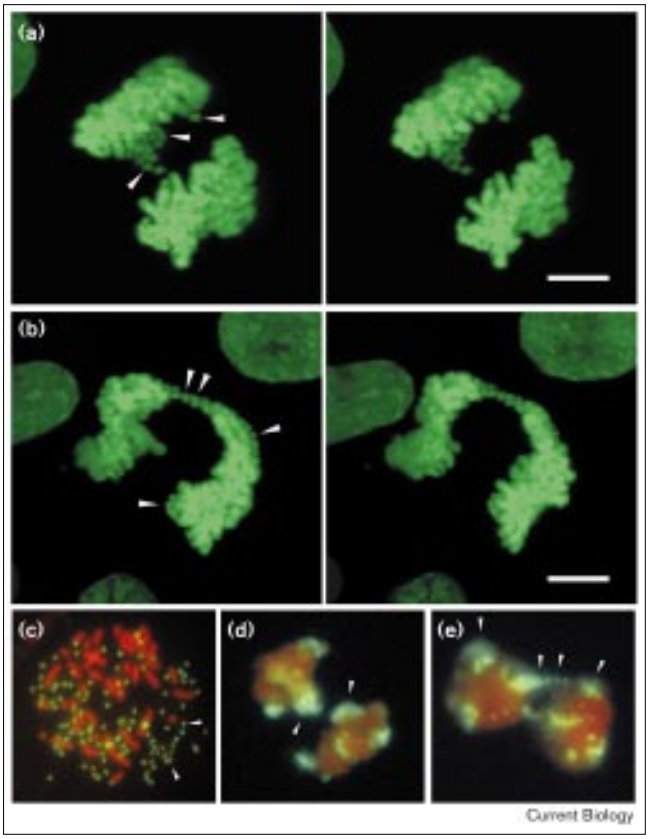

DMs cluster in anaphase cells. (a,b) Stereoscopic images of live COLO320DM cells expressing H2B–GFP. Clustered dot-like chromatin bodies (shown by arrowheads) together with segregating daughter chromosomes were visualized by GFP fluorescence (green). The scale bars are 5 μm. (c) DMs were detected in a metaphase spread of colcemid-treated COLO320DM cells by fluorescence *in situ* hybridization (FISH) using a biotinylated c-*myc* cosmid probe and fluoroscein-isothiocyanate–avidin. Chromosomes were counterstained with PI. (d,e) Asynchronously growing COLO320DM cells were directly fixed on chamber slides without colcemid treatment and processed for FISH analyses with the c-*myc* cosmid probe. Clustered DMs (arrowheads) and segregating daughter chromosomes (PI stained; red) are shown. Fluorescence images were collected using an epifluorescence microscope.

Figure 8

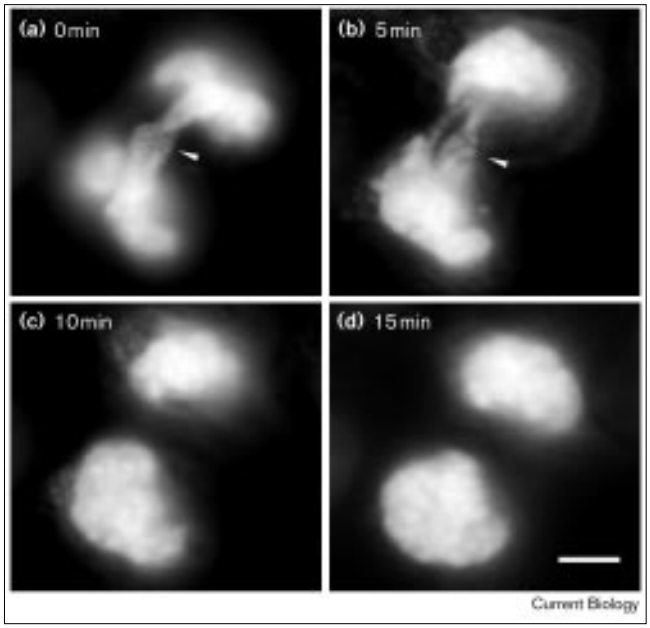

Transmission of DMs to daughter cells visualized in living cells. Time-lapse imaging of an H2B–GFP-labeled COLO320DM cell from late anaphase to telophase. A cluster of lagging DMs (shown by arrowheads) formed a bridge between segregating chromosomes, and the bridge was severed by cytokinesis. Fluorescence images were collected at the indicated times using an epifluorescence microscope equipped with a video camera. The scale bar is 5 μm.

H2B–GFP with mononucleosomes under high ionic strength (0.5 M NaCl). The primary interactions responsible for the stability of nucleosomes are electrostatic as nucleosomes can be dissociated into their DNA and histone components by elevating ionic strength. Histone H1, as well as non-histone proteins, dissociates from the nucleosomes at 0.5 M NaCl [7,19]. It is therefore likely that H2B–GFP protein is incorporated into nucleosome core particles rather than just affiliating with the core particles by a non-specific electrostatic interaction.

The strategy described in this paper offers significant advantages over other chromosome-labeling methods. Although fluorescent labeling of mammalian chromosomes in living cells has been demonstrated using Hoechst 33342 [26,27], each cell line must be analyzed individually to optimize the time of drug exposure and concentration of the drug [28]. Furthermore, as Hoechst 33342 is excited maximally near 350 nm and high intensities of ultraviolet (UV) irradiation can damage cells and produce cell cycle delay or arrest, the level of UV excitation must be controlled carefully. In addition, Hoechst 33342 affects cell cycle progression, arresting cells in G2 phase [29]. Intercalating DNA drugs, like dihydroethidium, may cause mutations in the DNA by interfering with DNA replication [28]. Microinjection of rhodamine-labeled histones, successfully used in *Drosophila* [8,9], is not suitable for analyzing a large population of mammalian cells. In contrast to these methods, the enhanced GFP [18] used in this study is excited with blue light (490 nm), which is less damaging than the UV-light excitation required for Hoechst. Moreover, constitutive expression of H2B–GFP from the integrated transgene enables long-term analyses without perturbing cell cycle progression (Figure 4). As the primary structures of histone proteins are well conserved among different species [30], it is likely that the H2B–GFP described here will be useful for cells of different species. This notion is supported by our ability to use the H2B–GFP vector in mouse, hamster, and monkey cells (data not shown).

The H2B–GFP strategy described in this report has a wide variety of applications for studying chromosome dynamics. For example, it can be used as a transfection marker that readily enables one to identify mitotic cells using fluorescence microscopy. H2B–GFP fluorescence persists in cells fixed in ethanol (Figure 4), which is useful for FACS analyses. As the intensity of H2B–GFP fluorescence depends on the chromosome condensation states in interphase cells (Figure 6), one can study chromosome condensation and decondensation in live cells [9]. The method may be especially useful for real-time analysis of apoptosis by enabling visualization of chromatin fragmentation and hypercondensation in living cells, as well as for studies of the effects of oncogenes on chromosome stability during tumor progression [31].

Using a retroviral vector expressing H2B–GFP, we have demonstrated that both normal chromosomes and small DMs can be readily distinguished in live cells. H2B–GFP enabled the observation of chromosomes in their native state without the need for fixation and permeabilization procedures, which can cause artificial distortion of intracellular structures. Our observations validate and extend a previous report in which DMs in fixed mitotic cells were observed to associate with the condensed chromosomes [5,6]. This led to a model for DM segregation involving 'hitch-hiking' of DMs on chromosomes [6]. The distinctive clustering behavior of DMs and their close association with normal chromosomes (Figures 7,8) provide one mechanism by which DMs are transmitted to daughter cells even though they lack functional centromeres. Clustered DMs appear to transmit to daughter cells in a highly stochastic manner, however. As COLO320DM cells grow faster when their levels of c-*myc* expression are elevated [4], daughter cells containing more DMs should be selected, and over time the population of cells will come to contain many DMs per cell. Therefore, although the number of DMs per cell is continuously changing by stochastic uneven distribution to daughter cells, DMs appear to be stably maintained when one considers the entire population. Sometimes, clustered DMs associate with both groups of the segregating daughter chromosomes, forming bridges across the midplane of anaphase cells (Figure 7b). It is tempting to speculate that such chromosomal bridges could increase chromosomal instability by inducing non-disjunction or, in some cases, by preventing chromosome segregation and increasing the probability of a chromosome arm being severed during cytokinesis. Were breakage to occur within an arm, genomic instability could be further increased by inheritance of the broken chromosome, which could initiate a bridge-breakage fusion cycle [32].

The mechanism of DM clustering during mitosis remains to be elucidated. One possibility is that DMs cluster due to their interaction with the spindle microtubules, as interaction of non-centromeric chromatin with the mitotic spindle is well documented [33]. Chromosome spreads of colcemid-treated cells reveal a scattered distribution of DMs (Figure 7c), suggesting that spindle microtubules may play an important role in DM clustering. Alternatively, DMs themselves may have cohesive properties and may 'stick' to each other. It has been reported that a hamster cell line containing large tandemly repeated amplicons including the dihydrofolate reductase gene also had anaphase-bridge formations due to delayed sister-chromatid disjunction [34]. Repeated arrays of amplicons in DMs may have configurations that favor DM clustering and delayed disjunction of sister minute chromosomes during anaphase. The interaction between DMs and normal chromosomes must be clarified as well. The H2B–GFP system described here should facilitate the additional analyses required to understand the precise mechanism of DM clustering and segregation.

Conclusions

We have established a novel system for labeling chromatin in living cells using a fusion protein of histone H2B and GFP. The H2B–GFP system allows chromosomes, including DMs, to be imaged at a high resolution without perturbing cell cycle control or intracellular structures. The application of this system has revealed the distinctive clustering behavior of DMs in living mitotic cells. We propose that DM clustering is an important factor leading to their asymmetric distribution to daughter cells.

Materials and methods

Construction of H2B–GFP expression vectors

A human *H2B* gene was obtained by PCR amplification of human placental genomic DNA using primers which introduce *Kpn*I and *Bam*HI sites at the ends of one of the reported H2B sequences (GenBank accession number X00088) [35]: primer 1, 5′-CGGGTACCGCCACCATGCCAGAGCCAGCGAAGTCTGCT-3′; primer 2, 5′-CGGGATCCTTAGCGCTGGTGTACTTGGTGAC-3′. Primer 1 introduced the Kozak consensus sequence in front of the initiation codon. PCR reaction parameters were as follows: 95°C for 10 min, 25 cycles at 94°C for 1 min, 50°C for 1 min, 72°C for 2 min, followed by 72°C for 5 min. One of the obtained clones, which was 98.4% identical to the H2B gene (X00088), was used to construct the H2B–GFP vector. The PCR product was digested with *Kpn*I and *Bam*HI and subcloned into the cloning site of pEGFPN1 vector (Clontech) [18]. The H2B–GFP chimeric gene was subcloned into a mammalian expression vector (J. Kolman, T.K., unpublished observations). H2B–GFP expression was driven by the EF-1α promoter, a strong promoter in mammalian cells [36]. The vector contained the blasticidin resistance gene [37] as a selection marker. A retroviral vector, pCLNC-H2BG, was constructed by cloning the H2B–GFP gene into the pCLNCX vector [38]. Cloning details are available upon request.

Cell lines and transfection

HeLa cells were grown as monolayers in Dulbecco's modified Eagle's medium (DMEM) supplemented with 10% fetal calf serum (FCS). Exponentially growing cells (in 10 cm dishes) were transfected with 20 μg H2B–GFP expression vector using a calcium phosphate precipitation protocol [39]. Transfected cells were replated 48 h after transfection and 5 μg ml^{-1} blasticidin-S (Calbiochem) was added 72 h after transfection. Five days later, the medium was changed to 2 μg ml^{-1} blasticidin-S. After 15 days of drug selection, surviving

colonies were checked under fluorescence microscopy and GFP-positive colonies were isolated. Several clones were selected and expanded into cell lines for further analyses. Production of VSV-G pseudotyped retrovirus [23] was performed by co-transfection of pCLNC-H2BG and pMD.G (the plasmid encoding the envelope protein VSV-G) into 293 gp/bsr cells as described [40]. COLO320DM cells [24] were grown in RPMI1640 medium supplemented with 10% FCS. Exponentially growing cells (in 10 cm dishes) were incubated with the concentrated viral supernatants in the presence of 8 μg ml^{-1} Polybrene (Aldrich). After overnight incubation, medium was changed and the infected cells were expanded for further analyses without drug selection.

Mononucleosome preparation

Mononucleosomes were purified according to the protocol (kindly provided by T. Ito and J. Kadonaga) [19] with several modifications. HeLa cells and stable cells expressing H2B–GFP (3×10^7) were trypsinized, harvested and washed once with 1× RSB buffer (10 mM Tris pH 7.6, 15 mM NaCl, 1.5 mM $MgCl_2$). After centrifugation, the cell pellet was resuspended in 1× RSB buffer with 1% Triton-X 100, homogenized by five strokes with a loose-fitting pestle to release nuclei. Nuclei were collected by centrifugation and washed twice with 1 ml buffer A (15 mM Tris pH 7.5, 15 mM NaCl, 60 mM KCl, 0.34 M sucrose, 0.5 mM spermidine, 0.15 mM spermine, 0.25 mM PMSF and 0.1% β-mercaptoethanol). Nuclei were finally resuspended in 1.5 ml buffer A and 15 μl 0.1 M $CaCl_2$ was added.

For making nucleosomal ladders, 0.5 ml suspended nuclei were digested by adding 1 μl micrococcal nuclease (Sigma, 200 units ml^{-1}) at 37°C. Aliquots (60 μl) were taken at each time point (1, 5, 10, 15, 30, 60 min) and 1.5 μl of 0.5 M EDTA was added to stop the reaction. To each tube, 18 μl H_2O, 12 μl 10% SDS and 24 μl 5 M NaCl were added. The mixtures were extracted with phenol–chloroform and 5 μl supernatant was analyzed by 1.5% agarose gel electrophoresis.

Limit digests for making mononucleosomes were performed by adding 10 μl micrococcal nuclease (200 units ml^{-1}) to 1.0 ml suspended nuclei. After 2 h digestion at 37°C, 20 μl 0.5 M EDTA was added to stop the reaction. The digest was centrifuged at 10,000 rpm for 10 min and the supernatant was collected. The pellet (chromatin fraction) was resuspended in 450 μl 10 mM EDTA, 50 μl 5 M NaCl was added to solubilize it, and the mixture was centrifuged at 14,000 rpm for 5 min to remove debris. The chromatin fraction was further fractionated on a 5–30% sucrose gradient for 18 h at 26,000 rpm in a Beckman SW41 rotor. After centrifugation, 1 ml fractions were collected and small aliquots (50 μl) of each sample were taken for DNA analyses. The remainder of each sample (950 μl) was precipitated with 280 μl 100% TCA with deoxycholic acid and left on ice for 10 min. The samples were then centrifuged at 3000 rpm for 5 min and each pellet was washed with acetone followed by a 70% ethanol wash. The pellet was air dried and resuspended in 20 μl of 1× SDS sample buffer, and aliquots were analyzed by gel electrophoresis through SDS–15% polyacrylamide gels followed by Coomassie staining. Western blotting was performed using anti-human-H2B antibody (1:1000, Chemicon) as a primary antibody. Signals were detected by enhanced luminol reagents (NEN Life Science Products) according to the manufacturer's instructions.

FACS analyses

HeLa cells and HeLa cells expressing H2B–GFP were harvested by trypsinization, fixed in 70% ethanol for 3 h at 4°C. Cells were stained with PI (20 μg ml^{-1}) containing RNase (200 ng ml^{-1}). Fluorescence was measured using a FACScan (Becton Dickinson). The red (PI) and green (GFP) emissions from each cell were separated and measured using standard optics. Color compensation was done to eliminate the artifact due to the overlap of PI and GFP emission. Cell debris and fixation artifacts were gated out. Data analysis was done using Cell Quest software (Becton Dickinson), and G1, S, and G2/M fractions were quantified using Multicycle software (Phoenix flow systems).

Fluorescence microscopy

For chromosome spreads, HeLa cells expressing H2B–GFP were treated with colcemid (100 ng ml^{-1}) for 1 h, trypsinized, harvested, and resuspended in hypotonic buffer (10 mM Tris pH 7.4, 10 mM NaCl, 5 mM $MgCl_2$; 1.5×10^6 cells ml^{-1}) for 10 min. Swollen cells (50 μl) were attached to poly-L-lysine coated slide glasses by cytospin (90 sec), fixed in 3.7% formaldehyde for 5 min, 0.1% NP40 in phosphate-buffered saline for 10 min and counterstained with DAPI (1 μg ml^{-1}). Images were collected with a Nikon fluorescence microscope equipped with either DAPI or fluoroscein isothiocyanate (FITC) filter sets.

Immunofluorescence with a human anti-centromere antiserum was performed as described previously [41]. Microscopy was performed on a BioRad 1024 confocal microscope built on a Zeiss Axiovert 100 using a 63× 1.4 NA Zeiss Plan Achromat objective lens.

FISH was performed as previously described using a biotinylated c-*myc* cosmid probe and FITC–avidin [25]. For *in situ* fixation, asynchronously growing COLO320DM cells were directly fixed on chamber slides (Lab-Tek) without colcemid treatment as described [31].

To visualize H2B–GFP in living cells, cells were grown on 25 mm coverslips and mounted with prewarmed culture medium in a Dvorak–Stotler chamber (Lucas-Highland Company). Images were collected on the BioRad 1024 confocal microscope described above using either the 63× lens or a 40× 1.3 NA Neofluar objective using a laser power of 0.3–1% for GFP fluorescence. Transmitted light images were collected with DIC optics. Fluorescence images were overlaid onto DIC images using Adobe Photoshop. Z-series images were collected and stereoscopic images were made using the BioRad software supplied with the microscope.

For time-lapse microscopy, cells were cultured in 35 mm glass-bottom culture dishes (Mat Tek Corporation). The culture medium was supplemented with 20 mM HEPES pH 7.3 and mineral oil was overlaid to cover the surface of the medium. The dishes were mounted on a Nikon inverted fluorescence microscope (Diaphot 300) equipped with a video camera (CCD72; MTI). The temperature of the medium was kept constant at 37°C using a heated stage. A 100× 1.3 NA oil-immersion lens was used for observation. Images were acquired using IP Lab spectrum software (Signal Analytics Corporation).

Acknowledgements

We thank J. Kolman for providing the backbone vector for H2B–GFP expression, F. Hanaoka for the blasticidin resistance gene, T. Ito and J. Kadonaga for the mononucleosome purification protocol, N. Somia and I. Verma for 293 gp/bsr cells, M. Friedlander and T. Hope for generously allowing us to use their microscopy systems, Wahl lab members for critically reading the manuscript and for their encouragement, R. Rubin for his helpful comments about nucleosomes, D. Chambers for the FACS analysis and M. Urista for her technical assistance. This work was supported by a grant from the Department of the Army, Grant number DAMD17-94-J4359 and by the G. Harold and Leila Y. Mathers Charitable Foundation (G.M.W.), and a grant from the National Institute for General Medical Sciences, GM39068 (K.F.S.).

References

1. Benner SE, Wahl GM, Von Hoff DD: Double minute chromosomes and homogeneously staining regions in tumors taken directly from patients versus in human tumor cell lines. *Anticancer Drugs* 1991, 2:11-25.
2. Cowell JK: Double minutes and homogeneously staining regions: gene amplification in mammalian cells. *Annu Rev Genet* 1982, 16:21-59.
3. Stark GR, Wahl GM: Gene amplification. *Annu Rev Biochem* 1984, 53:447-491.
4. Von Hoff DD, McGill JR, Forseth BJ, Davidson KK, Bradley TP, Van DD, *et al.*: Elimination of extrachromosomally amplified MYC genes from human tumor cells reduces their tumorigenicity. *Proc Natl Acad Sci USA* 1992, 89:8165-8169.

5. Barker PE, Hsu TC: Are double minutes chromosomes? *Exp Cell Res* 1978, 113:456-458.
6. Levan A, Levan G: Have double minutes functioning centromeres? *Hereditas* 1978, 88:81-92.
7. Wolffe A: *Chromatin: Structure and Function*, 2nd edn. San Diego: Academic Press; 1995.
8. Minden JS, Agard DA, Sedat JW, Alberts BM: Direct cell lineage analysis in ***Drosophila melanogaster*** by time-lapse, three-dimensional optical microscopy of living embryos. *J Cell Biol* 1989, 109:505-516.
9. Hiraoka Y, Minden JS, Swedlow JR, Sedat JW, Agard DA: Focal points for chromosome condensation and decondensation revealed by three-dimensional ***in vivo*** time-lapse microscopy. *Nature* 1989, 342:293-296.
10. Chalfie M, Tu Y, Euskirchen G, Ward WW, Prasher DC: Green fluorescent protein as a marker for gene expression. *Science* 1994, 263:802-805.
11. Cubitt AB, Heim R, Adams SR, Boyd AE, Gross LA, Tsien RY: Understanding, improving and using green fluorescent proteins. *Trends Biochem Sci* 1995, 20:448-455.
12. Gerdes HH, Kaether C: Green fluorescent protein: applications in cell biology. *FEBS Lett* 1996, 389:44-47.
13. Misteli T, Spector DL: Applications of the green fluorescent protein in cell biology and biotechnology. *Nat Biotechnol* 1997, 15:961-964.
14. Robinett CC, Straight A, Li G, Willhelm C, Sudlow G, Murray A, *et al.*: ***In vivo*** localization of DNA sequences and visualization of large-scale chromatin organization using lac operator/repressor recognition. *J Cell Biol* 1996, 135:1685-1700.
15. Straight AF, Belmont AS, Robinett CC, Murray AW: GFP tagging of budding yeast chromosomes reveals that protein-protein interactions can mediate sister chromatid cohesion. *Curr Biol* 1996, 6:1599-1608.
16. Shelby RD, Hahn KM, Sullivan KF: Dynamic elastic behavior of alpha-satellite DNA domains visualized ***in situ*** in living human cells. *J Cell Biol* 1996, 135:545-557.
17. Flach J, Bossie M, Vogel J, Corbett A, Jinks T, Willins DA, *et al.*: A yeast RNA-binding protein shuttles between the nucleus and the cytoplasm. *Mol Cell Biol* 1994, 14:8399-8407.
18. Yang TT, Cheng L, Kain SR: Optimized codon usage and chromophore mutations provide enhanced sensitivity with the green fluorescent protein. *Nucleic Acids Res* 1996, 24:4592-4593.
19. Laybourn PJ, Kadonaga JT: Role of nucleosomal cores and histone H1 in regulation of transcription by RNA polymerase II. *Science* 1991, 254:238-245.
20. Belmont AS, Bruce K: Visualization of G1 chromosomes: a folded, twisted, supercoiled chromonema model of interphase chromatid structure. *J Cell Biol* 1994, 127:287-302.
21. Moroi Y, Hartman AL, Nakane PK, Tan EM: Distribution of kinetochore (centromere) antigen in mammalian cell nuclei. *J Cell Biol* 1981, 90:254-259.
22. Bartholdi MF: Nuclear distribution of centromeres during the cell cycle of human diploid fibroblasts. *J Cell Sci* 1991, 99:255-263.
23. Burns JC, Friedmann T, Driever W, Burrascano M, Yee JK: Vesicular stomatitis virus G glycoprotein pseudotyped retroviral vectors: concentration to very high titer and efficient gene transfer into mammalian and nonmammalian cells. *Proc Natl Acad Sci USA* 1993, 90:8033-8037.
24. Alitalo K, Schwab M, Lin CC, Varmus HE, Bishop JM: Homogeneously staining chromosomal regions contain amplified copies of an abundantly expressed cellular oncogene (c-myc) in malignant neuroendocrine cells from a human colon carcinoma. *Proc Natl Acad Sci USA* 1983, 80:1707-1711.
25. Shimizu N, Kanda T, Wahl GM: Selective capture of acentric fragments by micronuclei provides a rapid method for purifying extrachromosomally amplified DNA. *Nat Genet* 1996, 12:65-71.
26. Belmont AS, Braunfeld MB, Sedat JW, Agard DA: Large-scale chromatin structural domains within mitotic and interphase chromosomes ***in vivo*** and ***in vitro***. *Chromosoma* 1989, 98:129-143.
27. Hiraoka Y, Haraguchi T: Fluorescence imaging of mammalian living cells. *Chromosome Res* 1996, 4:173-176.
28. Arndt-Jovin DJ, Jovin TM: Fluorescent labeling and microscopy of DNA. *Methods Cell Biol* 1989, 30:417-448.
29. Tobey RA, Oishi N, Crissman HA: Cell cycle synchronization: reversible induction of G2 synchrony in cultured rodent and human diploid fibroblasts. *Proc Natl Acad Sci USA* 1990, 87:5104-5108.
30. Wells DE: Compilation analysis of histones and histone genes. *Nucleic Acids Res* 1986, 14:R119-R149.
31. Denko N, Stringer J, Wani M, Stambrook P: Mitotic and post-mitotic consequences of genomic instability induced by oncogenic Ha-ras. *Somat Cell Mol Genet* 1995, 21:241-253.
32. Coquelle A, Pipiras E, Toledo F, Buttin G, Debatisse M: Expression of fragile sites triggers intrachromosomal mammalian gene amplification and sets boundaries to early amplicons. *Cell* 1997, 89:215-225.
33. Fuller MT: Riding the polar winds: chromosomes motor down east. *Cell* 1995, 81:5-8.
34. Warburton PE, Cooke HJ: Hamster chromosomes containing amplified human alpha-satellite DNA show delayed sister chromatid separation in the absence of ***de novo*** kinetochore formation. *Chromosoma* 1997, 106:149-159.
35. Zhong R, Roeder RG, Heintz N: The primary structure and expression of four cloned human histone genes. *Nucleic Acids Res* 1983, 11:7409-7425.
36. Mizushima S, Nagata S: pEF-BOS, a powerful mammalian expression vector. *Nucleic Acids Res* 1990, 18:5322.
37. Izumi M, Miyazawa H, Kamakura T, Yamaguchi I, Endo T, Hanaoka F: Blasticidin S-resistance gene (bsr): a novel selectable marker for mammalian cells. *Exp Cell Res* 1991, 197:229-233.
38. Naviaux RK, Costanzi E, Haas M, Verma IM: The pCL vector system: rapid production of helper-free, high-titer, recombinant retroviruses. *J Virol* 1996, 70:5701-5705.
39. Chen C, Okayama H: High-efficiency transformation of mammalian cells by plasmid DNA. *Mol Cell Biol* 1987, 7:2745-2752.
40. Miyoshi H, Takahashi M, Gage FH, Verma IM: Stable and efficient gene transfer into the retina using an HIV-based lentiviral vector. *Proc Natl Acad Sci USA* 1997, 94:10319-10323.
41. Sullivan KF, Hechenberger M, Masri K: Human CENP-A contains a histone H3 related histone fold domain that is required for targeting to the centromere. *J Cell Biol* 1994, 127:581-592.

Because *Current Biology* operates a 'Continuous Publication System' for Research Papers, this paper has been published on the internet before being printed. The paper can be accessed from http://biomednet.com/cbiology/cub – for further information, see the explanation on the contents page.